JACS
JOURNAL OF THE AMERICAN CHEMICAL SOCIETY
Communication
pubs.acs.org/JACS

Live Cell MicroRNA Imaging Using Cascade Hybridization Reaction

Zoya Cheglakov,[‡] Timothy M. Cronin,[†] Chuan He,*[,‡] and Yossi Weizmann*[,†]

[†]Department of Chemistry, The University of Chicago, 929 East 57th Street, Chicago, Illinois 60637, United States

[‡]Department of Chemistry and Institute for Biophysical Dynamics, The University of Chicago, 929 East 57th Street, Chicago, Illinois 60637, United States

Supporting Information

ABSTRACT: Recent advances in RNA research have posed new directives in biology and chemistry to uncover the complex roles of ribonucleic acids in cellular processes. Innovative techniques to visualize native RNAs, particularly, short, low-abundance RNAs in live cells, can dramatically impact current research on the roles of RNAs in biology. Herein, we report a novel method for real-time, microRNA imaging inside live cells based on programmable oligonucleotide probes, which self-assemble through the Cascade Hybridization Reaction (CHR).

The fundamental understanding of cellular processes in which microRNAs and other short RNA fragments are involved requires comprehensive and smart tools that allow visualization and localization of RNAs to be monitored in real-time under *in vivo* conditions. The use of the Fluorescent *In Situ* Hybridization (FISH) assay[1−3] is a prevailing method in cell biology for sensing DNA or RNA sequences in cells, tissues, and tumors. To date, *in situ* hybridization methods allow detection of nucleic acid samples using the programmable amplification for multiplexed imaging of mRNA.[4] Although, FISH-based techniques are productively used in a wide range of research areas,[5,6] dynamic visions of nucleic acids are required for a profound study of complex cell processes, such as chromatin organization and transcription regulation.[7−9] Specific hybridization techniques have been developed to permit the complete, *in vivo* labeling of chromatin or RNAs to gain a more complex view on nucleic acid dynamics within a living cell.[10] Other methods use fluorophore-tagged, oligonucleotide probes and are designed, conversely, to exclusively tag distinct chromatin regions or particular RNA species.[11,12]

Recently, numerous successful *in vivo* hybridization techniques based on oligonucleotide probes have been developed, demonstrating novel strategies in fluorescence detection and cell imaging fields.[13−17] The molecular beacons (MBs) approach has found wide application in mRNA analysis and may be used in a broad range of amplification methods, making nucleic acids a valuable instrument for molecular sensing. The use of MBs as a toolbox for biological applications offers numerous significant advantages. MBs' ability to sense specific DNA or RNA sequences with great accuracy, provided by the unique programmable nature of the loop-stem structure, leads to significantly improved efficiency and a high signal-to-noise ratio (SNR).[18,19] With careful design and optimized reaction conditions, nucleic acid probes may significantly increase the fluorescent intensity, producing a signal monitored directly as the hybridization event appears. Furthermore, chemical modifications applied to nucleic acid sequences offer considerably improved resistance to cellular endo- and exonucleases.[20] The efficiency of the delivery of nucleic acid probes into live cells is also a vital factor in the cell imaging procedure.[21] The distinctive combination of the MBs' properties may offer the unique ability to be used for many biological and medical applications: multiple-target detection in a single assay, real-time assaying, multiple cancer cells/cell lines, single base mutation sensing, and low-abundance miRNA sensing in live cells.

With this approach, we have developed a novel method based on programmable molecular hairpins[22−24] that produces repeated, binary-fluorescent, hairpin−hairpin duplexes as a result of cascading hybridization events triggered by a native RNA fragment inside live cells. RNA fragments act as reaction initiators and activate a Cascade Hybridization Reaction (CHR), constructing multiple DNA repeating units.[4] Each unit generates a Fluorescence Resonance Energy Transfer (FRET) signal.

Our method has been designed for sensing remarkably short (22 nucleotides) and low-abundance hsa-miR-21 microRNA target molecules. To date, microRNAs as target molecules are resilient to most visualization methods and remain a great challenge in the field of live-cell imaging. First, the short nature of miRNAs prevents signal amplification by multiple probes and requires an increase in the affinity of the probes in order to achieve detectable signals. Second, miRNAs can diffuse out of the cells during extended incubation and/or multiple washing processes. Furthermore, the expression level of a particular miRNA is different in various cell types, and in order to sense low-abundance microRNA molecules, selection of an isothermal, amplified, and highly accurate detection is required.

Our strategy is based on the use of two programmable DNA probes, hairpins HP_1 and HP_2. The HP_1 hairpin consists of loop fragment **2** and stem fragments **1** and **1′**. Due to the hybridization of the hsa-miR-21 molecule to the fragments **2** and **1**, HP_1 opens to reveal its stem fragment **1′**. Special design of HP_1 leads to the formation of a shared-stem duplex between the target and the fragments **1** and **2** (Scheme 1), constructing a highly stable complex, essential for the forward polymerization reaction between **1′** and HP_2 loop fragment **4** (Scheme 1). The repeating multiple hybridization reactions between HP_2 stem fragment **3** and HP_1 loop fragment **2** lead to the

Received: February 9, 2015
Published: May 1, 2015

DOI: 10.1021/jacs.5b01451
J. Am. Chem. Soc. 2015, 137, 6116−6119

Scheme 1. Illustration of the Cascade Hybridization Reaction

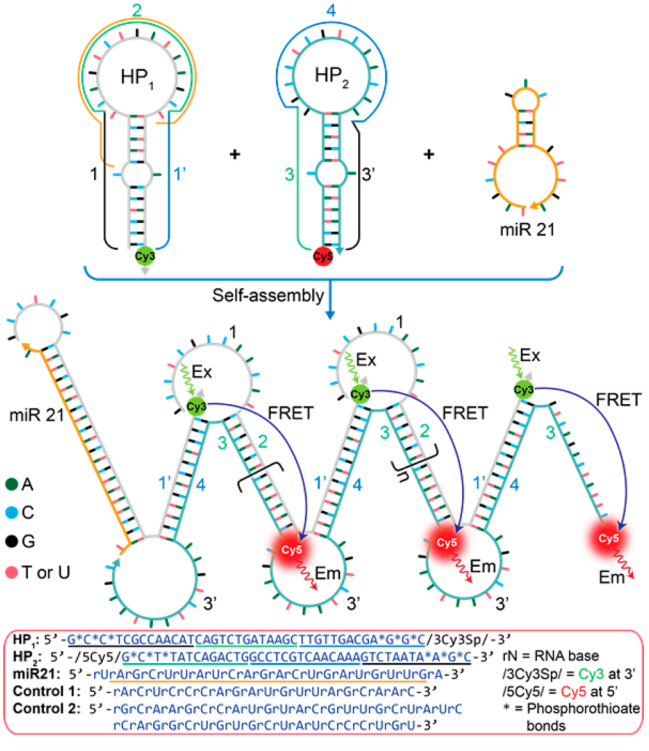

hybridization of HP_1 stem fragment **1**′ with HP_2 loop fragment **4** and offers a stage for a cascade reaction between HP_1 and HP_2 hairpins, accelerating the construction of a centipede-like structure (Scheme 1 and Figure S1). Each HP_1–HP_2 pair hybridization event leads to FRET signal generation. The hairpins stay metastable when no target is present, due to the closed formation of the hairpin stems. A FRET-based approach has been implemented in our system to prevent false positive signals that can be observed in quencher/dye systems as a result of probe accumulation and/or degradation.[25] The FRET CHR method is activated by a unique hybridization event between the hairpins and a target molecule, demonstrating high specificity and fast hybridization kinetics at 37 °C. Furthermore, the programmable character of nucleic acids offers a toolbox to image different native RNA target sequences inside live cells in real-time.

To verify our approach, we used *in situ* control experiments and nucleic acid designer computer programs[14] to quantify the hairpin stem and loop lengths necessary for the stability of the hybridization product units at physiological conditions.[15−17] First, the hairpins were designed in three different modes with variations programmed and introduced into the internal-stem part of the hairpin sequences. The optimal HP_1 and HP_2 DNA hairpins pair contained 15- and 14-nt loops, respectively, and 12-bp stems. Each hairpin was designed with a single internal mismatch in the stem region, to reduce the stability of an individual HP_1 or HP_2 compared to the generated DNA chain (Scheme 1). Full-stem-12-bp hairpins, as well as two-internal-mismatches-12-bp stem hairpins, were also designed and tested in-tube. The full-stem hairpins demonstrated very strong metastability properties resulting in complete blocking of the CHR, while two-internal-mismatches-12-bp stems' hairpins underwent hybridization in the absence of the target molecule (Figures S3 and S4). Second, HP_1 acts as the architect linker in the hairpin-target tandem and provides a platform for the HP_2 to bridge the HP_1–target hybrid and to trigger the subsequent hybridization reaction (Scheme 1, Figures S1 and S2). Therefore, an excess of HP_1 leads to a significant improvement of the CHR acceleration, higher reaction efficiency, and, as a result, higher signal-to-background ratio. By doubling the HP_2 concentration, we succeeded in increasing the number of generated fluorescent hybrid units from 5 to 15 (Figure S5, lane 1). Further examination of the hairpins led to the conclusion that the optimal ratio of the HP_1 and HP_2 hairpins is 2:1, respectively (Figure S5, lane 2). In contrast to the effect of the ratio findings, the order in which the hairpins entered the system showed no influence on the CHR results (Figure S6e and S6f).

To retrieve optimal conditions for further live-cell experiments we performed a number of *in vitro* tests. FRET analysis was applied to reveal the metastability properties of the hairpin pairs, as well as to confirm CHR selectivity (Figure 1a). The

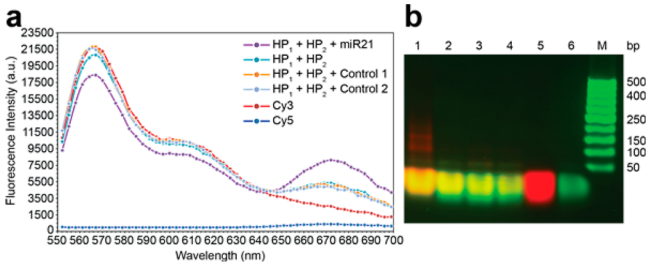

Figure 1. (a) In-tube FRET analysis: HP_1 donor, HP_2 acceptor with hsa-miR-21 target (purple line); HP_1 donor, HP_2 acceptor (cyan line); HP_1 donor, HP_2 acceptor with *β*-actin negative control 1 (orange line); HP_1 donor, HP_2 acceptor with Son DNA negative control 2 (light blue line); HP_1 donor (Cy3, red line); HP_2 acceptor (Cy5, blue line). 100 nM HP_1 and 100 nM HP_2 was reacted with 10 nM of hsa-miR-21 target/negative controls. (b) Agarose gel analysis: HP_1, HP_2 with hsa-miR-21target (lane 1); HP_1, HP_2 with Son DNA negative control 2 (lane 2); HP_1, HP_2 with *β*-actin negative control 1 (lane 3); HP_1, HP_2 mixture (lane 4); HP_2 (lane 5); HP_1 (lane 6). 100 nM HP_1 and 100 nM HP_2 was reacted with 10 nM of hsa-miR-21 target/negative controls.

mixtures of HP_1 and HP_2 demonstrated strong metastability properties without the hsa-miR-21 target (blue line) and underwent CHRs in the presence of the hsa-miR-21 molecule (purple line). *β*-actin and Son DNA sequence fragments, used as negative controls (orange line and light blue line, respectively), showed low signals, analogous to the hairpins-only mixture. Gel-electrophoresis analysis was performed to support FRET results and to validate the number of the generated fluorescent units (Figure 1b). Hairpins HP_1 and HP_2 showed strong metastability properties individually (lanes 6 and 5, respectively) and in the absence of the hsa-miR-21 target (lane 4). Lanes 3 and 2 corresponding to negative control fragments *β*-actin and Son DNA, respectively, exhibited a lack of the CHR event. Lane 1 shows ladder shaped bands when hsa-miR-21 is present, indicating successful CHR.

As different expression levels of miR-21 have been recognized to demonstrate sensitivity to various anticancer agents,[26] miR-21 has been indicated as an "oncomir" or a miRNA with oncogenic effects.[26] In light of this evidence, we applied our method to investigate hsa-miR-21 miRNA in numerous mammalian cell lines.[27] Human epithelial carcinoma cancer (HeLa) live cells, known to express relatively high levels

DOI: 10.1021/jacs.5b01451
J. Am. Chem. Soc. 2015, 137, 6116−6119

of miR-21 miRNA, were analyzed using CHR assay and characterized by a laser scanning confocal system. Cell areas were imaged using two different confocal planes and demonstrated clear signals indicating the presence of free hsa-miR-21 in live HeLa cells and offered distinct localization of the signals within each cell (Figures 2a, 2b and S6). To evaluate the

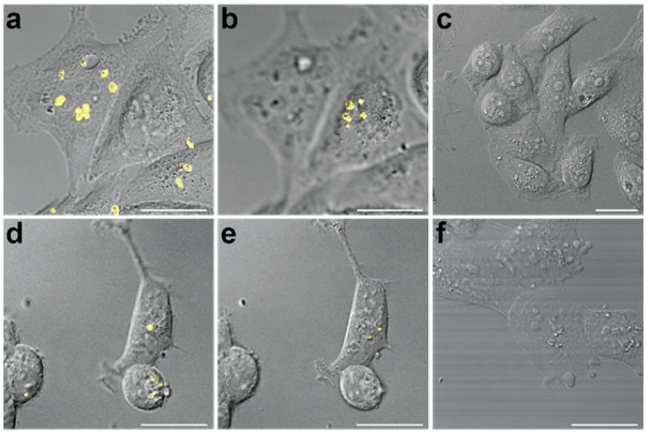

Figure 2. Live-cell FRET analysis. (a, b) HeLa live cells in the presence of HP_1, HP_2 mixture after 4 h CHR, two confocal planes of the same area were imaged for 2 min with a time interval of 60 s. (c) HeLa live cells in the presence of chemically modified AMOs showed specific inhibition of hsa-miR-21. (d, e) HEK293 live cells were monitored in two confocal planes of the same area for 2 min with a time interval of 60 s and showed a low hsa-miR-21 expression level. (f) MRC-5 cell line control experiment demonstrates no hsa-miR-21. Scale bar = 25 μm.

effectiveness of CHR on cell lines with high and low miR-21 expression profiles, the method was applied to different cell types and controls. When the hsa-miR-21 expression in HeLa live cells was knocked down by the anti-miRNA antisense inhibitor oligodeoxyribonucleotides (AMOs),[27,28] no FRET signal was observed (Figures 2c and S10). Human embryonic kidney cells (HEK293) exhibiting a relatively low miR-21 expression profile were monitored at two confocal planes of the same area showing the comparatively reduced presence of hsa-miR-21 (Figures 2d, 2e and S7). Considering that hsa-miR-21 is a cancer biomarker, we used human normal lung fibroblast (MRC-5) cells as a noncancerous/negative control (Figure 2f). CHR efficiency was supported by the lifetime studies (Figures S8 and S9). Further, confocal fluorescence microscopy was used to image a series of z-sections through the entire HeLa cells. 3D z-stack projections were taken following CHR in the presence of the HP1, HP2 mixture to localize the hsa-miR-21 molecules throughout the entire HeLa live cell (Figures 3 and S12).

In summary, the vital role of miRNA in cell regulation processes and its association with various human cancers as a tumor suppressor or an oncogenic fragment indicate great demand for an accurate and rapid approach for highly efficient miRNA imaging in live cells. Here, we demonstrate an approach using two programmable nucleic acid sequences, labeled with either a donor or an acceptor fluorophore dye. The CHR strategy is a one-step method, capable of sensing the molecule of interest in a reaction solution, avoiding complicated separation of the excess materials. The nucleic acids can be designed and aimed at native miRNAs and generate sharp, cascade FRET signals as a result of the unique

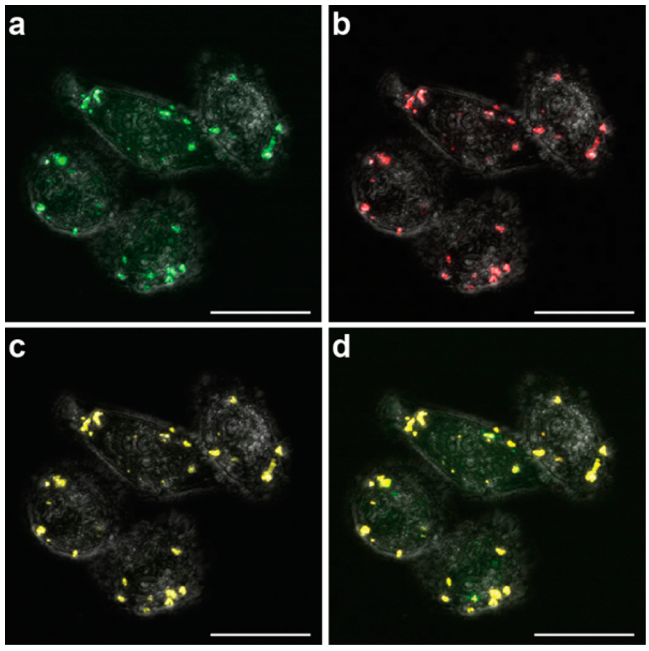

Figure 3. FRET analysis of HeLa cells z-stacks: (a) Green channel: donor excitation 543 and 575 nm donor emission, related to Cy3 fluorescent; (b) the red channel: 633 nm acceptor excitation/680 nm acceptor emission, related to Cy5 fluorescent dye. (c) FRET channel (donor excitation 543 nm/680 nm acceptor emission, FRET). (d) Merged images a, b, c. Z-stack projections were made of 47 slices stacks at 0.2 μm increments of the entire HeLa cells after 4 h CHR at 37 °C. Scale bar = 25 μm.

hybridization event. Our method offers a programmable, fluorescent, amplification toolbox that can be applied to any miRNA target of interest in a live cell, in real-time. The increased material diffusion provided by the hairpin probes and the triggered self-assembly character of the method offer a high signal-to-noise ratio. Precise signal localization at the level of a single live cell is achieved as a result of the tethering method. The Cascade Hybridization Reaction (CHR) system has been proven to be viable for the detection of lowly expressed, short RNA targets within a few hours. When submitting this work, we believe that the capability to visualize and localize any desired endogenous RNA in a live cell, in real-time, may offer new possibilities in biological and medical analysis.

■ ASSOCIATED CONTENT

Supporting Information

Experimental details and additional characterization data. The Supporting Information is available free of charge on the ACS Publications website at DOI: 10.1021/jacs.5b01451.

■ AUTHOR INFORMATION

Corresponding Authors

*chuanhe@uchicago.edu
*yweizmann@uchicago.edu

Notes

The authors declare no competing financial interest.

■ ACKNOWLEDGMENTS

All the confocal images and z-stack 3D projection studies were carried out in the Integrated Microscopy Core Facility at the University of Chicago.

DOI: 10.1021/jacs.5b01451
J. Am. Chem. Soc. 2015, 137, 6116–6119

REFERENCES

(1) Qian, X.; Jin, L.; Lloyd, R. V. *J. Histotechnol.* **2004**, *27*, 53.
(2) Wagner, M.; Horn, M.; Daims, H. *Curr. Opin. Microbiol.* **2003**, *6*, 302.
(3) Amann, R.; Fuchs, B. M. *Nat. Rev. Microbiol.* **2008**, *6*, 339.
(4) Choi, H. M.; Chang, J. Y.; Trinh, L. A.; Padilla, J. E.; Fraser, S. E.; Pierce, N. A. *Nat. Biotechnol.* **2010**, *28*, 1208.
(5) Silverman, A.; Kool, E. *Adv. Clin. Chem.* **2007**, *43*, 79.
(6) Lawrence, J. B.; Singer, R. H.; Marselle, L. M. *Cell* **2004**, *57*, 493.
(7) Thisse, B.; Heyer, V.; Lux, A.; Alunni, V.; Degrave, A.; Seiliez, I.; Kirchner, J.; Parkhill, J.; Thisse, C. *Methods Cell Biol.* **2004**, *77*, 505.
(8) Denkers, N.; Garcia-Villalba, P.; Rodesch, C. K.; Nielson, K. R.; Mauch, T. *J. Dev. Dynam.* **2004**, *229*, 651.
(9) Hocine, S.; Raymond, P.; Zenklusen, D.; Chao, J. A.; Singer, R. H. *Nat. Methods.* **2013**, *10*, 119.
(10) Goodell, M. A.; Godley, L. A. *Blood* **2013**, *121*, 5131.
(11) Santangelo, P. J.; Nix, B.; Tsourkas, A.; Bao, G. *Nucleic Acids Res.* **2004**, *32*, 1.
(12) Molenaar, C.; Marras, S. A.; Slats, J. C.; Truffert, J. C.; Lemaitre, M.; Raap, A. K.; Dirks, R. W.; Tanke, H. J. *Nucleic Acids Res.* **2001**, *29*, E89.
(13) Tyagi, S.; Kramer, F. R. *Nat. Biotechnol.* **1996**, *14*, 303.
(14) Zadeh, J. N.; Steenberg, C. D.; Bois, J. S.; Wolfe, B. R.; Pierce, M. B.; Khan, A. R.; Dirks, R. M.; Pierce, N. A. J. *Comput. Chem.* **2011**, *32*, 170.
(15) Park, H. Y.; Lim, H.; Yoon, Y. J.; Follenzi, A.; Nwokafor, C.; Lopez-Jones, M.; Meng, X.; Singer, R. H. *Science* **2014**, *343*, 422.
(16) Seferos, D. S.; Giljohann, D. A.; Hill, H. D.; Prigodich, A. E.; Mirkin, C. A. *J. Am. Chem. Soc.* **2007**, *129*, 15477.
(17) Wu, P.; Hwang, K.; Lan, T.; Lu, Y. *J. Am. Chem. Soc.* **2013**, *135*, 5254.
(18) Feldkamp, U.; Niemeyer, C. M. *Angew. Chem., Int. Ed.* **2006**, *45*, 1856.
(19) Feldkamp, U.; Niemeyer, C. M. *Angew. Chem., Int. Ed.* **2008**, *47*, 3871.
(20) Egli, M.; Pallan, P. S. *Chem. Biodivers.* **2010**, *7*, 60.
(21) Boutorine, A. S.; Novopashina, D. S.; Krasheninina, O. A.; Nozeret, K.; Venyaminova, A. G. *Molecules* **2013**, *18*, 15357.
(22) Drake, T. J.; Tan, W. *Appl. Spectrosc.* **2004**, *58*, 269A.
(23) Zhu, S.; Wu, H.; Wu, F.; Nie, D.; Sheng, S.; Mo, Y. Y. *Cell Res.* **2008**, *18*, 350.
(24) Tsourkas, A.; Behlke, M. A.; Bao, G. *Nucleic Acids Res.* **2002**, *30*, 5168.
(25) Bao, G.; Rhee, W. J.; Tsourkas, A. *Annu. Rev. Biomed. Eng.* **2009**, *11*, 25.
(26) Alahar, S. *MicroRNA in Cancer* **2013**, *VIII*, 148.
(27) Kumarswamy, R.; Volkmann, I.; Thum, T. *RNA Biol.* **2011**, *8*, 706.
(28) Lu, Y.; Xiao, J.; Lin, H.; Bai, Y.; Luo, X.; Wang, Z.; Yang, B. *Nucleic Acids Res.* **2009**, *37*, 1.

DOI: 10.1021/jacs.5b01451
J. Am. Chem. Soc. 2015, 137, 6116−6119